Article

Development of a P84/ZCC Composite Carbon Membrane for Gas Separation of H_2/CO_2 and H_2/CH_4

Nurul Widiastuti,* Alvin Rahmad Widyanto, Irmariza Shafitri Caralin, Triyanda Gunawan,
Rika Wijiyanti, Wan Norharyati Wan Salleh, Ahmad Fauzi Ismail, Mikihiro Nomura, and Kohei Suzuki

Read Online

ACCESS | Metrics & More | Article Recommendations | Supporting Information

ABSTRACT: Hydrogen (H_2) has become one of the promising alternative clean energy resources. Membrane technology is a potential method for hydrogen separation or production. This study aims to develop a new carbon membrane for hydrogen separation or production. Moreover, the permeation behavior of H_2, CO_2, and CH_4 through a hollow fiber composite carbon membrane derived from P84 co-polyimide and with incorporation of zeolite composite carbon (ZCC) was also examined. ZCC was synthesized via the impregnation method of sucrose into zeolite-Y pores, followed by carbonization at 800 °C. Thus, this filler has a high surface area, high microporosity, ordered pore structure, and low hydrophilicity. The presence of zeolites in ZCC is predicted to increase certain gases' affinity for the membrane. Various heating

rates (1−5 °C/min) were applied during pyrolysis to understand the effect of the heating rate on the pore structure and H_2/CO_2 and H_2/CH_4 gas separation performance. Moreover, gas permeation was evaluated at various temperatures (298−373 K) to study the thermodynamic aspect of the process. A characteristic graphite peak was detected at $2\theta \sim 44°$ in all carbon samples. Scanning electron microscopy (SEM) observations revealed the void-free surface and the asymmetric structure of the carbon membranes. During the permeation test, it was found that gas permeation through the membrane was significantly affected by the temperature of the separation process. The highest permeability of H_2, CO_2, and CH_4 was detected on the composite carbon membrane at a 3 °C/min heating rate with a permeation temperature of 373 K. The thermodynamic study shows that CO_2 and H_2 have lower activation energies compared to CH_4. The transport mechanism of the membrane involved adsorption and activated surface diffusion. The permeation temperature has a large impact on the transport of small penetrants in the carbon matrix.
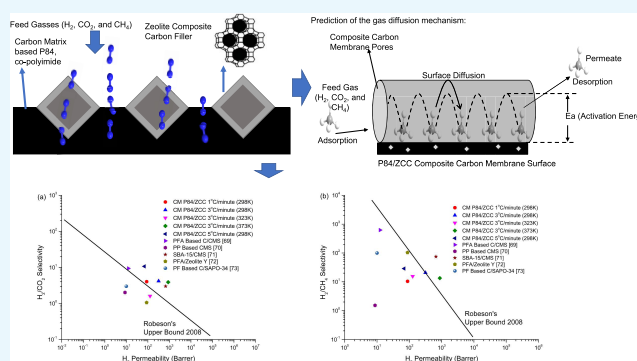
1. INTRODUCTION

Hydrogen has become one of the promising alternative clean energy resources. The increase in demand for hydrogen as clean energy in the upcoming decade has been predicted following the Paris Conference of the Parties (COP) agreement in limiting the global temperature rise to "well below 2 °C".[1] Among all hydrogen production technologies, the gas steam reforming process is widely used for hydrogen production by converting methane (CH_4) into hydrogen (H_2).[2] However, in this process, not all methane gas can be converted properly into hydrogen gas and so the produced gas contains impurities. Thus, separation of hydrogen and methane is important.

Another final product of gas stream reforming is carbon dioxide (CO_2) gas. Carbon dioxide is well known as a greenhouse gas that can contribute to global warming due to its highest retention time and greatest rate in the atmosphere.[3] Carbon dioxide is also produced from hydrogen production by the syngas process, followed by the water gas shift (WGS) reaction, which mainly consists of a mixture of 45% H_2 and

30% CO_2.[4] In this process, further separation of H_2 and CO_2 is required.

Currently, major technologies for CO_2 separation are amine absorption and cryogenic distillation, which are energy- and cost-intensive processes.[5] Pressure swing adsorption (PSA) is commonly used for H_2 purification.[6] The major drawback of this method is low energy efficiency consumption.[7] The membrane technology process has attracted the attention of researchers because of its low investment cost, simple operation, and highly efficient energy consumption,[8] thus making it a promising candidate for the process. Moreover, as technology advances, a better separation performance is in demand; thus, a novel membrane needs to be developed.
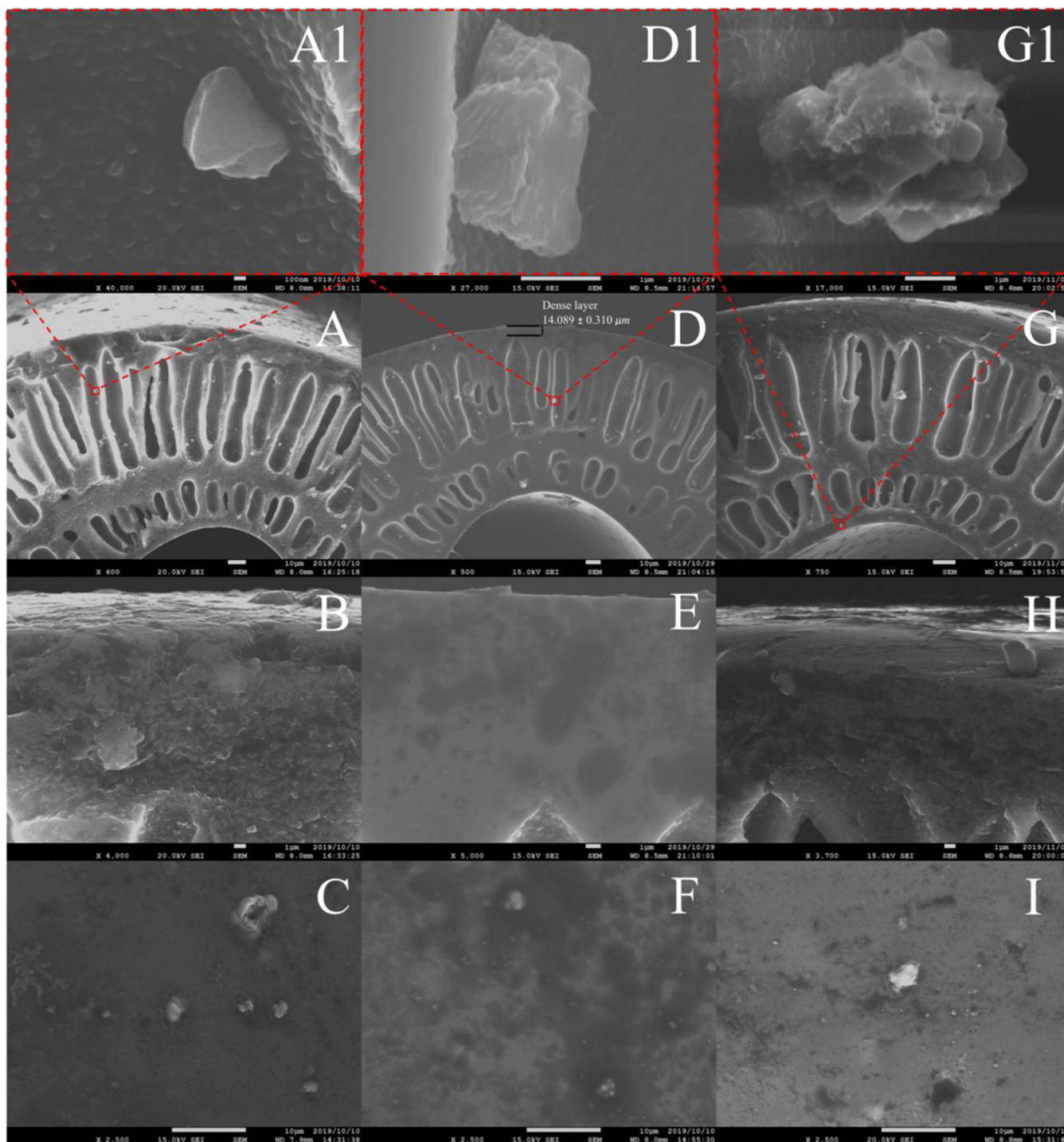
Figure 1. FESEM morphology of P84/ZCC composite carbon membranes at various heating rates: (cross section, (A); (B); and (A1) zoom-in of (A) and surface, (C)) 1 °C/min, (cross section, (D); (E); and (D1) zoom-in of (D) and surface, (F)) 3 °C/min, and (cross section, (G); (H); and (G1) zoom-in of (G) and surface, (I)) 5 °C/min.

Based on the literature, inorganic membranes have superior stability compared with polymeric membranes.[9] Among inorganic membranes, zeolite membranes,[10−13] metallic membranes,[14−17] carbon membranes,[18−21] and silica membranes[22−24] are the most studied for gas separation. Among them, carbon membranes offer the simplest manufacturing process and have superior thermal and chemical stability. Moreover, the gas separation performance is excellent.[18,25] Carbon membranes are usually produced via carbonization of a polymeric precursor under vacuum or inert gas atmospheres and at high temperatures ranging from 500 to 700 °C.[26] The polymeric precursor selection plays an important role in the final pore structure of the carbon membrane.[27] Glassy polymers such as polyimide (PI) and their derivates have been widely used in preparing carbon membranes due to their well-rounded features.[28−34] Moreover, membrane module selection, such as a hollow fiber carbon membrane, showed good hydrogen separation performance for H_2/CO_2 and $H_2/$

CH$_4$.[35−37] In this study, carbon membranes were produced from P84 co-polyimide as the main precursor due to its excellent separation performance.[38]

In addition to the precursor selection, the heating rate during the carbonization process is an important factor in determining the separation properties of the carbon membrane. Based on previous research, Favvas et al. reported that low heating rates resulted in low gas permeation.[39] Suda and Haraya reported increasing permeability of the produced carbon membrane by applying a higher heating rate of carbonization.[40] The heating rate also influences the pore structure and the characteristic of the resulting carbon membrane.[41,42] The heating rate treatment is commonly used in the range of 1−13 °C/min, while the most effective heating rate was in the range of 1−5 °C/min.[26] Thus, in this study, the carbon membranes were carbonized at various heating rates of 1−5 °C/min. Moreover, the effect of permeation temperature in the range of 30−100 °C was also investigated to understand the thermodynamic aspect of the studied membrane.

Enhancement of the carbon membrane performance by adding filler particles has received a lot of attention in recent years. Inorganic particles, such as silica,[43] zeolite,[44] and carbon molecular sieve,[45] are widely used as carbon membrane fillers. Using inorganic fillers on membranes can lead to formation of cracks on the membrane surface due to formation of separate phases or microvoids along with the barrier of the phase fill interface in the carbon matrix.[46] Previously, we have also studied a new type of filler on a mixed matrix membrane (MMM), which is zeolite composite carbon (ZCC).[47,48] Our results showed that addition of ZCC on the P84 polymeric membrane could enhance the permeability and selectivity performance of CO$_2$/CH$_4$ and O$_2$/N$_2$. ZCC was synthesized via impregnation of sucrose inside the zeolite pores. Sucrose was selected as it provides a high carbon yield, which is suitable for microporous carbon preparation.[49] Moreover, addition of a carbon layer inside the zeolite pore hinders the attraction of moisture that leads to permeability reduction and reduces the pore size to 7.29 ± 0.04 Å.[47,48,50] This material has potential as a filler for carbon membranes because of its regular pore structure, high micropore site, and compatibility as carbon membrane filler particles. The presence of zeolites in ZCC is thought to increase certain gases' affinity for the membrane, resulting in better permeation. Addition of ZCC in the P84 membrane increased the permeability for CO$_2$ (1791%) and CH$_4$ (585%).[47] In our previous study, addition of ZCC improved both permeabilities of O$_2$ and N$_2$ and O$_2$/N$_2$ selectivity by 121, 165, and 81%, respectively, of the P84/ZCC mixed matrix membrane.[32] Thus, this study aims to develop a composite hollow fiber carbon membrane derived from P84/ZCC MMMs for H$_2$ purification.

The work continues previous research to provide insight into the fundamentals of carbon membrane by investigating characteristics at a variety of heating rate temperatures. A comprehensive understanding of permeation of gases through carbon membranes is essential to elucidate the adsorption properties. Thus, the purpose of this study was to improve the performance of co-polyimide carbon membranes with the ZCC filler at various heating rates during carbonization. This parameter is tested to determine the characteristics of the membrane and its effect on membrane performance. Besides, this research also studies the improvement of membrane performance by varying the operating temperature during the

permeation and membrane selectivity testing process, as well as studying the thermodynamic aspects of the gas separation process and the process of the gas transport mechanism through the membrane.

2. RESULTS AND DISCUSSION

2.1. Membrane Characterization. *2.1.1. Morphological Structure of Composite Carbon Membranes.* The prepared carbon membranes at the various heating rates were investigated using field emission scanning electron microscopy (FESEM) to study membrane morphology. Figure 1A,B,D,E,G,H shows the cross-sectional morphology of the carbon membrane at various heating rates. The morphological profile of the P84/ZCC composite carbon membrane shows that it consists of two outer and inner layers with a porous fingerlike sublayer in between. This structure was obtained as a result of phase inversion between coagulation liquid and polymer solution during the dry/wet-spinning process.[26] These membrane structures are similar to the previously reported membrane with the P84 co-polyimide polymeric material.[32] This shows that there was no structural damage due to stabilized precursors at 300 °C under N$_2$ atmospheric conditions. All prepared carbon membranes show defect-free surfaces (Figure 1C,F,I) and an asymmetric pore structure with a dense layer on the top and fingerlike pores in the substructure (Figure 1A,B,D,E,G,H) similar to the mixed matrix membrane from our previous study.[47,48] The carbonization process in the polymer membrane produces an amorphous carbon structure due to the destruction of the C−H bond.[26] Addition of the ZCC filler into the carbon matrix shows good dispersion, as can be seen in Figure 1 of the cross section and the surface morphology of the composite carbon membrane.

The dense layer data of P84/ZCC composite carbon membranes at various heating rates of 1, 3, and 5 °C/min is shown in Table 1. The dense layer thickness of the hollow fiber

Table 1. Dense Layer Data of the P84/ZCC Composite Carbon Membrane at Various Heating Rates

heating rates in P84/ZCC carbon membrane (°C/min)	dense layer of P84/ZCC carbon membrane (μm)
1	13.520 ± 0.094
3	14.089 ± 0.310
5	14.510 ± 0.201

carbon membrane was measured using ImageJ software with at least five-point measurements from several scanning electron microscopy (SEM) images of corresponding membranes.[51] The heating rate treatment plays a major role in formation of carbon structures on membranes. As reported by Sazali et al., the higher the heating rate of carbonization, the denser the carbon membrane.[52]

Based on our previous study, the filler composition could affect the orientation of the filler on the membrane surface.[53] A total of 1 wt % filler gives the ideal orientation of the filler position on the membrane surface. In this study, we use a 1 wt % filler composition assuming that it has similar properties. Illustration of ZCC into carbon matrix-based P84 is displayed in Figure 2.

2.1.2. Microstructure Composite Carbon Membranes. In fabrication of carbon membranes influenced by heating rate protocols, the heating rate becomes one of the main
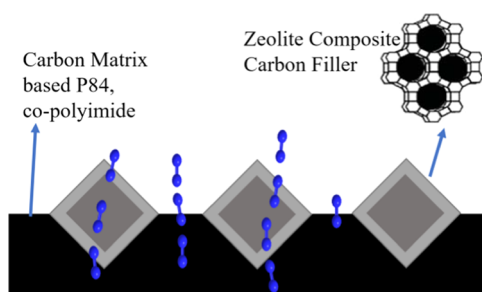
Figure 2. Illustration introduction of ZCC into carbon matrix-based P84.

contributions to the carbon structure formation.[54] The heating rate influences the evolution rate of volatile components from the polymer structure when pyrolyzing a polymeric membrane. Typically, volatile byproducts may include ammonia (NH_3), hydrogen cyanide (HCN), methane (CH_4), hydrogen (H_2), nitrogen (N_2), carbon monoxide (CO), and others, depending on the polymer.[55] The heating rate also represents the time of the sample exposed to heat, which afterward works on the reaction and diffusion processes.[56]

X-ray diffraction (XRD) characterization was performed to examine the phase of the microstructure and the distance between layers (d-spacing) of the carbon membrane as an effect of the carbonization heating rate. The distance between layers exhibits a gas diffusion path on the carbon membrane.[57,58] XRD diffractograms of carbon membranes are shown in Figure 3. Diffractograms of all carbon membranes contained an amorphous structure (002) and aromatic graphite (100) at 2θ of about 22 and 42°.[59]

Compared to the precursor polymeric membrane, a carbon membrane with a denser structure was obtained by decreasing the d-spacing value. The polymeric precursor membrane has a d-spacing value of 4.98 Å after the pyrolysis process with a variety of heating rates. The P84 carbon membrane has a d-spacing value of 3.94 Å. The d-spacing value at 2θ (about 22°) of the P84/ZCC composite carbon membrane was lower than that of the P84 carbon membrane. This was caused by the presence of ZCC, which creates a more regular structure. P84/ZCC carbon membranes have a d-spacing value in a sequence with the heating rates (1, 3, and 5 °C/min) of 3.67, 3.93, and 3.84 Å, respectively. The value of d-spacing on carbon membranes approaches the d-spacing value of graphite, 0.335 nm.[60]

The P84/ZCC carbon membrane at the heating rate of 1 °C/min showed the smallest d-spacing value compared to the amorphous structure phase (002) at other heating rates. This was caused by a slow pyrolysis process at a low heating rate due to the slower release of volatile components. Therefore, the produced carbon membrane has a more regular structure. The higher the heating rate, the quicker the pyrolysis process. The increasing heating rates of carbonization contribute to the increasing d-spacing value of the carbon membrane owing to the faster volatile component release. As a result, an imperfect graphite structure was formed; thus, the d-spacing value was greater.[42] However, the unique pattern was obtained at 5 °C/min. Based on the XRD spectra at the carbonization heating rate of 5 °C/min, it is seen that the peak is shifted to the right, with the result that there appears to be a decrease in the d-spacing value.[61] The d-spacing value represents the dimension of space for a small gas molecule to penetrate through a
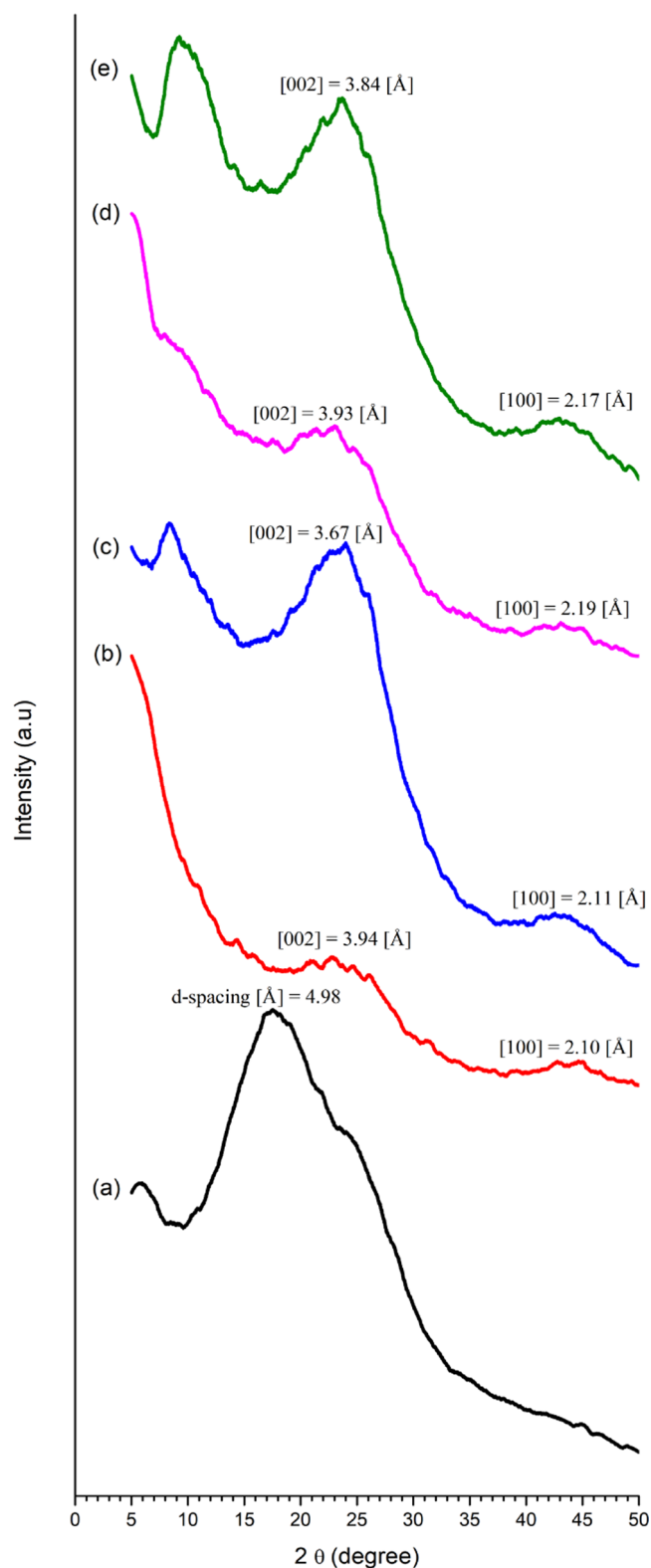
Figure 3. XRD pattern of (a) polymeric precursor membrane, (b) P84 carbon membrane, and the P84/ZCC composite carbon membrane at various heating rates of (c) 1 °C/min, (d) 3 °C/min, and (e) 5 °C/min, respectively.

membrane, and this data provides helpful information to determine the permeability and the selectivity of a membrane supported by other analyses. Sazali et al. reported that a decrease in the d-spacing value results in narrow pore sizes.[62]

The slight decrease of the average *d*-spacing of the carbon membranes contributed to a great molecular sieving effect.[40,62] The existence of a 2θ peak at around 42° indicates an aromatic graphite phase, showing that the amorphous carbon structure has changed to aromatic carbon graphite. As a result, the carbon membrane was predicted to have a high selectivity.[63,64]

The study by Su and Lua reports an uncommon trend that occurs due to the influence of the heating rate on gas permeability.[65] Increasing the heating rate may or may not increase certain gases' permeability. The improvement in permeability of He and CO_2 was found by increasing the heating rate from 0.5 to 4 °C/min, but for N_2, permeability reduction occurred, and the permeability of O_2[65] was not affected.[65]

2.1.3. Pore Character of the Composite Carbon Membrane. Pore size distribution (PSD) from the N_2 adsorption–desorption isotherm data was carried out using SAIEUS software with the two-dimensional (2D) nonlocal density functional theory (NLDFT) model.[50] Figure 4 shows the PSD
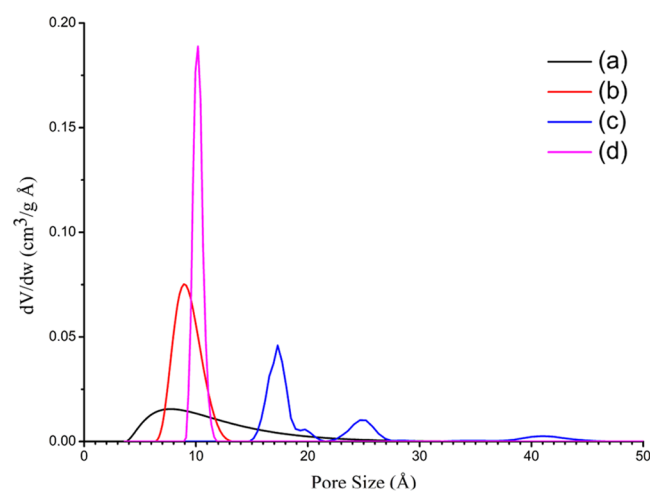

Figure 4. Pore size distribution of (a) P84 carbon membrane and the P84/ZCC composite carbon membrane at heating rates of (b) 1 °C/min, (c) 3 °C/min, and (d) 5 °C/min.

of the prepared membranes. The pore size plays an important role in determining the gas diffusion mechanism in the P84/ZCC composite carbon membranes. Pore size distribution analysis was expected to describe the type of gas diffusion occurring on the P84/ZCC composite carbon membranes. Generally, carbon membrane with mesopores (2–50 nm pore diameter), micropores (pore diameter ≤2 nm), and ultra-micropores (pore diameter ≤0.6 nm) follow the gas diffusion mechanism of Knudsen diffusion, surface adsorption, and molecular sieving, respectively.[66] The addition of ZCC as a filler in the carbon membrane can create a more ordered pore structure. The P84/ZCC composite carbon membrane at the heating rate of 1 °C/min has the smallest pore size with an average pore size of 0.897 nm. This result confirms the results of X-ray diffraction (XRD) of the P84/ZCC *d*-spacing value. The carbonization process occurs slowly with less pressure, resulting in a carbon membrane with a more regular structure.[42]

The P84/ZCC composite carbon membrane treated at a heating rate of 3 °C/min has micropores at 1.5–2 nm, as well as has mesopores at 2.1–2.8 nm, and about 4 nm with small intensity, respectively. The average pore size of the composite

carbon membrane was 1.729 nm. The increasing heating rates of carbonization contribute to the increasing pore size of the carbon membrane owing to the faster volatile component release. A similar result was reported by Xu et al., where an increase of the heating rate of carbonization from 1 to 3 °C/min contributed to the increasing pore size and deformation occurring on the pores of the carbon membrane.[41] Besides, the higher pore size supported the increasing *d*-spacing data from 1 to 3 °C/min, which interconnected. The presence of mesoporous composite carbon membranes corresponded to the incomplete structural arrangement of graphite.[42]

The P84/ZCC composite carbon membrane at a heating rate of 5 °C/min possesses a micropore size with an average pore size of 1.01 nm. The unique result of pore size distribution becomes sharper in the micropore area, and a decreasing mesopore was also reported previously.[67] The higher heating rate during pyrolysis leads to the loss of the mesopores and an almost complete shift to a microporous carbon product. The enhancement of the micropore area with a narrow diameter is caused by the collapse of the micro/mesoporous structure during the carbonization process.[67] Moreover, increasing the heating rate from 3 to 5 °C/min enhances the microporosity percentage from 31.8 to 44.2%.[67] This supports the smaller *d*-spacing data compared to composite carbon membranes at a heating rate of 3 °C/min. Decreasing in *d*-spacing value affects molecular sieving properties.[40] Besides, the micropores on the composite carbon membrane at a heating rate of 5 °C/min had the highest intensity because the graphite phase on the carbon membrane had a more regular structure.

In several previous studies, it has been stated that the characteristics of the pore structure of porous inorganic membranes have a strong influence in determining the gas permeation diffusion mechanism.[68–70] The porous inorganic membrane having a pore of 0.5–2 nm was the limit of the diffusion mechanism that works between molecular sieving and Knudsen diffusion and/or surface diffusion.[71] The diffusion mechanism of composite carbon membranes based on pore size at heating rates of 1 and 5 °C/min was surface diffusion (selective adsorption) because the pore diameter of the carbon membrane was in the micropore range.[66] Composite carbon membranes at a heating rate of 3 °C/min have the diffusion mechanism as a combination of surface diffusion (selective adsorption), because of the presence of micropores, and Knudsen diffusion as a result of the presence of mesopores.[66]

The N_2 adsorption–desorption isotherms are shown in Figure 5 and Table 2. the P84/ZCC composite carbon membranes prepared at heating rates of 1 and 5 °C/min indicate type 1 isotherm, while carbon membranes at the heating rate of 3 °C/min indicate type IV according to the International Union of Pure and Applied Chemistry (IUPAC).[72] Type 1 refers to pore filling at low pressure in the presence of an increase in adsorbent–adsorptive interactions in very narrow pores (close to molecular dimensions), indicating that the carbon membrane has micropores. On the other hand, the carbon membrane at the heating rate of 3 °C/min shows type IV, which is indicated by not being filled directly with pores at low pressure due to adsorption occurring in mesoporous pores consisting of multilayer adsorption followed by pore condensation. The heating rate of the carbon membrane affects the resulting pore structure, supporting XRD data, where the carbon membrane
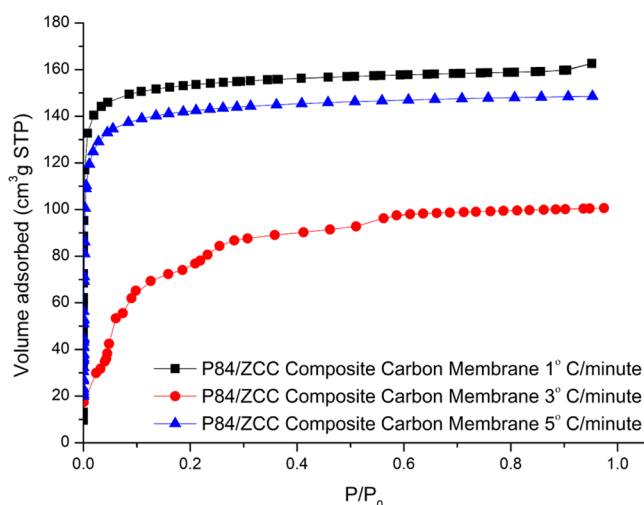
Figure 5. Isothermal adsorption of the P84/ZCC composite carbon membranes.

Table 2. N$_2$ Adsorption Parameters of the Composite Carbon Membrane

parameter	P84/ZCC composite carbon membrane		
	1 °C/min	3 °C/min	3 °C/min
S$_{BET}$ (m^2/g)	606.990	373.040	568.320
α_s plot of micropore area (m^2/g)	615.987	268.092	615.208
α_s plot of external surface area (m^2/g)	9.173	1.758	3.332
total pore volume (cc/g)	0.252	0.153	0.228
average pore size (nm)	0.897	1.729	1.010

with a heating rate of 3 °C/min has the highest d-spacing value, which indicates the presence of mesopores.

2.1.4. Thermal Stability of the Composite Carbon Membrane. The P84/ZCC composite carbon membranes that have been prepared at various heating rates were also analyzed using thermal gravimetric analysis (TGA) in a N$_2$ gas environment to determine the thermal stability of the carbon membrane. The TGA curve is shown in Figure 6. In all composite carbon membranes, decomposition occurs at a temperature of 100 °C by 8−11%, which indicates moisture evaporation on the composite carbon membrane.[73]

The P84/ZCC composite carbon membranes have good thermal stability as indicated by the 5−9% amount of mass lost up to a temperature of 800 °C. The good thermal stability of the P84/ZCC composite carbon membranes shows the potential to be applied on a large scale. In addition, the heating rate affects the stability of the P84/ZCC composite carbon membrane. This is indicated by the percentage of mass lost from the P84/ZCC composite carbon membrane at various heating rates in the following order: 1 °C/min (18.6% decomposed) > 3 °C/min (15.8% decomposed) > 5 °C/min (14.5% decomposed). The higher the heating rate, the lesser the percentage of mass lost. This shows that the produced P84/ZCC composite carbon membrane is more stable.

2.2. Carbon Membrane Separation Performance at Various Heating Rates.

The P84/ZCC carbon membrane was tested for the performance of H$_2$/CO$_2$ and H$_2$/CH$_4$ gas separation at various heating rates. The gas separation results of the P84/ZCC carbon membrane with the effect of the heating rate are shown by the permeability and the selectivity values in Table 3. For the P84/ZCC carbon membrane, the gas
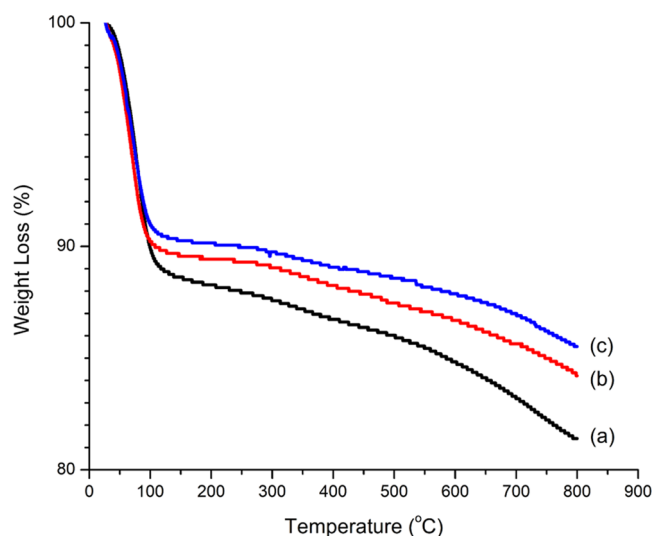

Figure 6. TGA curve of the P84/ZCC composite carbon membrane at various heating rates of (a) 1 °C/min, (b) 3 °C/min, and (c) 5 °C/min.

permeability values of H$_2$, CO$_2$, and CH$_4$ at a 1 °C/min heating rate were 88.14, 21.9, and 8.47 barrer, and the selectivity values of H$_2$/CO$_2$ and H$_2$/CH$_4$ gas pairs were 4.03 and 10.41, respectively. In addition, the gas permeability values of H$_2$, CO$_2$, and CH$_4$ at a 3 °C/min heating rate were 315.84, 75.39, and 15.25 barrer, and the selectivity values of the H$_2$/CO$_2$ and H$_2$/CH$_4$ gas pairs were 4.19 and 20.71, respectively. The P84/ZCC carbon membrane at a 5 °C/min heating rate had H$_2$, CO$_2$, and CH$_4$ gas permeability values of 69.03, 6.46, and 2.39 barrer, and the selectivity values of H$_2$/CO$_2$ and H$_2$/CH$_4$ gas pairs were 10.69 and 28.86, respectively.

This research also studied the effect of pyrolysis temperature on the gas separation performance of the P84/ZCC carbon membrane at various heating rates, as shown in Table 3. The permeability of all gases for the carbon membrane was higher than that of the mixed matrix membrane (MMM) P84/ZCC. The dominant gas transport mechanism on the carbon membrane is molecular sieving.[20] Gas diffusivity in carbon membranes depends on the size and diameter of the gas molecules because the pore size of the membrane is close to the dimensions of the gas molecules.[74] H$_2$, CO$_2$, and CH$_4$ gas permeability trends depend on the kinetic diameter of the gas. The order of gas permeability from highest to lowest was H$_2$ (0.289 nm) > CO$_2$ (0.33 nm) > CH$_4$ (0.38 nm).

The heating rate in pyrolysis controls the rate of evolution of the volatile components of the polymer membrane during carbonization and affects the microstructure of the resulting carbon membrane.[26] The permeability and selectivity performance of the gas pair (H$_2$/CO$_2$ and H$_2$/CH$_4$) on the carbon membrane with the influence of the heating rate is shown in Figure S1a,b. The order of gas permeability values with the effect of the heating rate is as follows: 3 °C/min > 1 °C/min > 5 °C/min. At a heating rate of 3 °C/min, the highest increase in gas permeability was for H$_2$ (315.62 barrer, 258.34% increase), CO$_2$ (75.39 barrer, 244.25% increase), and CH$_4$ (15.25 barrer, 80.05% increase). This trend is the same as that reported by Sazali et al., where the carbonization heating rate of the polyimide (PI)/nanocrystalline cellulose (NCC) membrane at 3 °C/min has the highest CO$_2$ and N$_2$ permeation values; then, on increasing the heating rates of

Table 3. Gas Separation Performance of the Carbon Membranes

membrane	permeability (barrer)			selectivity	
	H_2	CO_2	CH_4	H_2/CO_2	H_2/CH_4
CM P84/ZCC 1 °C/min at 298 K	88.14 ± 8.99	21.9 ± 0.34	8.47 ± 0.40	4.03	10.41
CM P84/ZCC 3 °C/min at 298 K	315.84 ± 21.31	75.39 ± 10.72	15.25 ± 4.17	4.19	20.71
CM P84/ZCC 3 °C/min at 323 K	126.91 ± 6.62	79.25 ± 1.22	8.16 ± 0.35	1.60	15.55
CM P84/ZCC 3 °C/min at 373 K	879.91 ± 59.75	225.78 ± 80.43	65.43 ± 3.01	3.90	13.45
CM P84/ZCC 5 °C/min at 298 K	69.03 ± 46.47	6.46 ± 2.33	2.39 ± 0.37	10.69	28.86
PFA based C/CMS[78]	12.48	1.33	0.02	9.38	624.00
PP based CMS[79]	8.7	4.3	5.7	2.02	1.53
SBA-15/CMS[80]	667.5	222.5	8.9	3.00	75.00
PFA/zeolite-T[81]	87.9	83.1	0.85	1.06	103.41
PF based C/SAPO-34[82]	10	8.7	0.1	3.00	100.00
Knudsen selectivity[37]				4.69	2.83

carbonization by 5 °C/min, the permeation value decreased.[52] Increasing the rate of carbonization heating can affect the pore size distribution by producing smaller pores. Moreover, it can cause other restrictions in the degrees of freedom of gas rotation.[75,76] Figure S1a,b shows the increase of gas pair selectivity with the increasing rate of carbonization heating. The carbonization heating rate of 5 °C/min had the highest increase in gas pair selectivity in H_2/CO_2 (10.69, 165.26% increase) and H_2/CH_4 (28.86, 177.23% increase). This is because the polymer-based carbon membrane with a smaller pore size can be obtained by a higher heating rate of carbonization. In addition, an increase in the heating rate can lead to the appearance of microscopic holes and cracks on the membrane surface.[77] The diffusion mechanism of the H_2/CO_2 and H_2/CH_4 gas pairs was also reviewed with the Knudsen selectivity, where Knudsen diffusion occurs due to molecular collision against the pore wall and Knudsen selectivity is obtained from the root ratio value of the molecular weight of each gas pair.[75] In the H_2/CH_4 gas pair, the selectivity value is 3−10 times the Knudsen selectivity (2.83) of all carbon membranes, which indicates that the diffusion mechanism occurs due to surface diffusion (selective adsorption). In the H_2/CO_2 gas pair, the selectivity value of the carbon membrane at the heating rate of 5 °C/min was two times that of the Knudsen selectivity (4.69). The dominant diffusion mechanism that occurs is surface diffusion (selective adsorption). However, carbon membranes with heating rates of 1 and 3 °C/min showed a lower selectivity value than the Knudsen selectivity on H_2/CO_2 separation.

2.3. Carbon Membrane Separation Performance Influenced by Permeation Temperature. The P84/ZCC carbon membrane produced at a heating rate of 3 °C/min (at the optimum heating rate) was then tested for its performance toward permeability and selectivity for H_2/CO_2 and H_2/CH_4 at operating temperatures of 298, 323, and 373 K to understand the thermodynamic properties of the membrane. The results are listed in Table 3. The performance of the carbon membrane treated at 3 °C/min heating rate and at various permeation temperatures is shown in Figure S2. The P84/ZCC carbon membrane at a 3 °C/min heating rate and a permeation temperature of 298 K exhibits H_2, CO_2, and CH_4 permeability values of 315.84, 75.39, and 15.25 barrer, respectively. On the other hand, the H_2/CO_2 and H_2/CH_4 selectivities were 4.19 and 20.71, respectively. Gas permeability values at 323 K of H_2, CO_2, and CH_4 were 126.91, 79.25, and 8.16 barrer, respectively, while the H_2/CO_2 and H_2/CH_4 selectivities were 1.60 and 15.55, respectively. Gas permeability

values at 373 K of H_2, CO_2, and CH_4 were 879.91, 225.78, and 65.43 barrer, respectively, and the H_2/CO_2 and H_2/CH_4 selectivities were 3.90 and 13.45, respectively. The operating temperature during permeation has an influence on the gas separation performance in the carbon membrane.[83] The increase of temperature during permeation affects the properties of gas adsorption on the carbon membrane, which has a surface diffusion mechanism (selective adsorption).[84] The gas permeability patterns of H_2, CO_2, and CH_4 on carbon membranes at various temperatures also depend on the kinetic diameter of the gas. The following is the order of gas permeability from the highest to the lowest: H_2 (0.289 nm) > CO_2 (0.33 nm) > CH_4 (0.38 nm).

Separation of the mixture gas (H_2/CO_2 and H_2/CH_4) was evaluated at various permeation temperatures of 298, 323, and 373 K, as shown in Figure S2a,b. Permeation at room temperature (298 K) had permeability values for H_2, CO_2, and CH_4 of 315.84, 75.39, and 15.25 barrer, respectively, and the selectivities of H_2/CO_2 and H_2/CH_4 were 4.19 and 20.71, respectively. Gas permeation at 323 K decreased the permeability of H_2 (−59.82%), CO_2 (−48.69%), and CH_4 (−46.50%). However, there was an improvement in the permeability of CO_2 (5.12%), followed by a reduction in the selectivity of H_2/CO_2 (−61.78%) and H_2/CH_4 (−24.89%). Permeation at 323 K has a unique pattern because the overall gas permeability decreases. However, when the permeation temperature was higher (at 373 K), the permeability of all H_2, CO_2, and CH_4 gases was obtained as 178.60, 199.47, and 329.03%, respectively. This fact contributes to the selectivity performance of H_2/CO_2 and H_2/CH_4 mixture gases, which were decreased by −6.97 and −35.06%, respectively.

The permeability of CO_2 gas increases with the permeation temperature. This is because the diffusivity of CO_2 increases with the increase of temperature, which has the same pattern as those of other studies.[37,85] In addition, for other gases that have decreased permeation at 323 K, this unique pattern is the same as that in the study reported by Favvas et al. that used a carbon membrane from co-polyimide precursors at various permeation temperatures of 313, 333, and 373 K.[37] At 333 K, the permeability is lower. These results are also supported by other micromembranes in addition to carbon membranes such as zeolite-MFI membranes in the studies of Au et al.,[86] Bernal et al.,[87] Lai and Tsapatsis,[88] and Poshusta et al.[89] In general, an increase of temperature is followed by an increase of permeation in the micropore membrane, beyond the minimum limit at a certain temperature, and then at a higher temperature, the permeation further increases.

There are two types of competition mechanisms in the micropore membrane: adsorption and surface diffusion. Both of the mechanisms are affected by the permeation temperature. Micropores contribute to mass transport, in which gas molecules jump between adsorption sites. Increasing the temperature results in an increase in the activated and diffusivity processes but a decrease in the extent of adsorption and the occupancy rate.[37] This assumption is used for permeation at 323 K, where a decrease in the occupancy occurs due to decreasing permeation. When the temperature increases during permeation at 373 K, the adsorption effect is negligible. The molecules in the pores maintain their gaseous property and pass through from one site to another by overcoming the energy barrier.[37] The diffusion mechanism is called translational diffusion and involves the micropore structure. The prediction of the diffusion mechanism is illustrated in Figure 7.
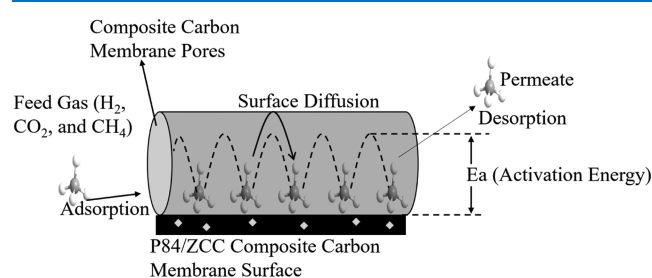

Figure 7. Prediction of the gas diffusion mechanism in the P84/ZCC composite carbon membranes.

The permeation performance was also supported by thermodynamics and activation energy data, which were calculated via van't Hoff and Arrhenius equations. The studied parameters involve enthalpy (ΔH), entropy (ΔS), and the change in Gibbs free energy (ΔG) obtained from eq 1. Plotting $\ln(p/p_0)$ versus $1/T$ gave a slope corresponding to ΔH and an intercept equal to ΔS (Table 4).

The heat of adsorption (enthalpy) confirms the strength of the interactions among adsorbent and adsorbate,[50] where the adsorbate is a gas (H_2, CO_2, and CH_4) and the adsorbent is the active surface site in the carbon membrane. The enthalpy (ΔH) values of CO_2 and CH_4 were negative (−16.68 and −20.60 kJ/mol). The negative enthalpy outcomes exhibit that the adsorption of these gases on the carbon membrane was

exothermic. Meanwhile, H_2 gas had a positive enthalpy value (54.69 kJ/mol). The positive enthalpy results indicated that the adsorption of this gas on the carbon membrane was endothermic. The enthalpy yield was not greater than 80 kJ/mol, which shows that the adsorbate and adsorbent interactions are influenced by physisorption.[90] Physisorption does not involve chemical bonds but is more dependent on the difference between the dipoles on the surface of the adsorbent (membrane surface) and the atoms in the adsorbate (gas molecules). The volume of adsorbate covering the surface is low, causing a strong interaction between adsorbate and adsorbent.[50] This argument can be applied to permeation at 323 K. The membrane transport mechanism is activated surface adsorption and diffusion. Therefore, the decrease of H_2 gas permeability (−59.82%) was higher than that of CH_4 (−46.50%) due to the enthalpy value (ΔH) of H_2, which was greater than CH_4. This causes a reduction in the selectivity of H_2/CH_4 gas separation (−24.89%). In addition, the permeability of CO_2 gas increased at 323 K. This result was inversely proportional to the decreased H_2 gas permeability, which contributed to decreasing H_2/CO_2 selectivity (−61.78%). This was because the CO_2 gas at the operating temperature increases in quantity, indicating its greater diffusivity. These results were the same as those of other studies.[37,85,91] As a result, the selectivity value of H_2/CO_2 was also decreased by −61.78%.

The entropy value (ΔS) in each gas (H_2, CO_2, and CH_4) is 0.35, 0.14, and 0.14 kJ/mol, respectively. A positive value of entropy indicates the increase of irregularity at the gas interface during permeation.[92] This shows that H_2, CO_2, and CH_4 gases have the mobility for diffusion into the carbon membrane pores. The smallest molecular size of H_2 gas contributes to the highest gas entropy value.

The change in Gibbs free energy (ΔG) of all gases shows a negative value, which is shown in Table 4. A negative result implies that a spontaneous adsorption process occurred in the permeation membrane.[50] The increase in temperature at permeation was followed by an increase in Gibbs free energy, indicating that at higher temperatures at permeation, gas adsorption was more spontaneous. However, at 373 K, the adsorption is negligible. Permeability is more influenced by the activation energy or energy barrier.[37]

The activation energy is a barrier to the diffusion energy of surface activation. Higher activation energy has a higher

Table 4. Thermodynamic Parameters and Energy of Activation for Permeation of H_2, N_2, and CH_4

membranes	gas	ΔH (kJ/mol)	ΔS (kJ/mol)	ΔG (kJ/mol)	E_a (kJ/mol)
P84/ZCC composite carbon membrane (3 °C/min)	H_2	54.69	0.35	−50.14 (298 K)	15.13
				−58.93 (323 K)	
				−76.52 (373 K)	
	CO_2	−16.68	0.14	−61.23 (298 K)	14.21
				−57.34 (323 K)	
				−60.75 (373 K)	
	CH_4	−20.60	0.16	−67.57 (298 K)	20.15
				−64.81 (323 K)	
				−71.66 (373 K)	
PIM-EA(H_2)-TB[93]	H_2	−4.6			0.5
	CO_2	−16.7			8.6
	CH_4	−4.8			13.1
carbon molecular sieve 6FDA/DETDA:DABA[94]	CO_2	−7.7			16.6
	CH_4	−7.0			19.2

tendency to penetrate the micropores. In this research, the activation energy values were determined using eq 2, as shown in Table 4. The sequence of activation energies is CO_2 (14.21 kJ/mol) < H_2 (15.13 kJ/mol) < CH_4 (20.15 kJ/mol). Activation energy affects permeation at 373 K. Permeability increases sequentially as CH_4 > CO_2 > H_2. The value of the increase in CO_2 is higher than that of H_2 due to the insignificant difference in activation energy. Surface diffusion from one site to another depends on the difference in dipoles on the surface of the adsorbent. The presence of zeolite in the alkaline form (Na) in the zeolite-carbon composite (ZCC) filler increases the affinity of CO_2 gas due to acid−base reactions.[81] Therefore, the increase in CO_2 permeability is higher than that of H_2, which results in the decrease of H_2/CO_2 selectivity (−6.97%). The value of the increase in permeability of CH_4 (329.03%) was higher than that of H_2 (178.60%) because the value of the activation energy of CH_4 was higher than that of H_2; thus, the selectivity of H_2/CH_4 was decreased by −35.06%.

The gas separation results of H_2/CO_2 and H_2/CH_4 compared to the Robeson curve are shown in Figure 8. Almost all carbon membranes, except for CM P84/ZCC at a

Figure 8. Gas separation performance of (a) H_2/CO_2 and (b) H_2/CH_4 when compared with other literature data.[78−82] with respect to the Robeson upper bound curve.[95]

heating rate of 3 °C/min at 323 K, had good H_2/CO_2 gas separation results, which were over the Robeson upper bound, and also show better performance compared to other studies.[78−82] CM P84/ZCC at a heating rate of 3 °C/min and at 298 and 373 K showed good H_2/CH_4 separation performance.

3. CONCLUSIONS

A P84/ZCC composite carbon membrane has been successfully prepared via the pyrolytic process. The carbon formation was confirmed using XRD and FESEM analysis. The XRD pattern shows a typical peak of amorphous structure (002) and aromatic graphite (100) at 2θ of about 22 and 42°. The XRD result confirms the SEM image that shows a defect-free surface and an asymmetric structure of the membrane. Carbonization conditions at various heating rates (1, 3, and 5 °C/min) were used to study the effect of the heating rate on H_2/CO_2 and H_2/CH_4 gas separation performance. The increasing heating rate produces better selectivity, which at 5 °C/min has the highest selectivity. The highest permeability was found at 3 °C/min due to the presence of mesopores. The diffusion mechanism was a combination of adsorption and activated surface diffusion. Different permeation temperatures result in thermodynamic and activation energy. The gas permeability at 323 K was low owing to the adsorption properties' contribution. The enthalpy (ΔH) values of H_2, CO_2, and CH_4 were 54.69, −16.68, and −20.60 kJ/mol, respectively, which suggested a stronger adsorption effect on H_2 than CH_4 at 323 K. When the temperature increases during permeation to 373 K, the adsorption effect is negligible. Activation energy affects permeation at 373 K; the sequence of activation energies is CO_2 (14.21 kJ/mol) < H_2 (15.13 kJ/mol) < CH_4 (20.15 kJ/mol). Permeability increases sequentially as follows: CH_4 > CO_2 > H_2. Almost all carbon membranes show good H_2/CO_2 gas separation performance, which is above the Robeson upper bound. The highest H_2/CH_4 separation performance was found for the CM P84/ZCC membrane with a heating rate of 3 °C/min at temperatures of 298 and 373 K.

4. MATERIALS AND METHODS

4.1. Materials. The carbon membrane was prepared using a P84 membrane, P84/ZCC mixed matrix membrane, and ultra-high-purity N_2 gas (99.99% N_2). An epoxy resin; P84 carbon membrane; and ultra-high-purity H_2, CO_2, and CH_4 gases (99.99%) were used for the gas permeation tests. The reasons for the selection of these materials are described in Table 5.

4.2. Methods. *4.2.1. Preparation of the P84/ZCC Carbon Membrane.* Preparation of zeolite composite carbon (ZCC) can be found elsewhere.[47] Sucrose was impregnated into zeolite-Y pores with a molar ratio of 12.5:10, followed by pyrolysis at 800 °C. Preparation of the P84 and the P84/ZCC mixed matrix membranes was carried out using a method previously reported by Widiastuti et al.[48] Then, P84 and P84/ZCC membranes underwent carbonization by a N_2 pyrolysis process. Initially, the pyrolysis conditions involved stabilization at 300 °C for 1 h, which was achieved at a heating rate of 3 °C/min. Subsequently, the temperature was increased to the final pyrolysis temperature of 700 °C over 1 h at a heating rate of 3 °C/min. Lastly, the membrane was allowed to cool naturally to room temperature.
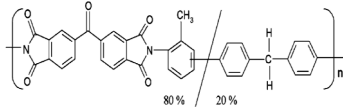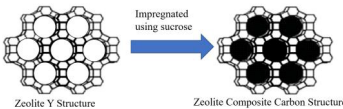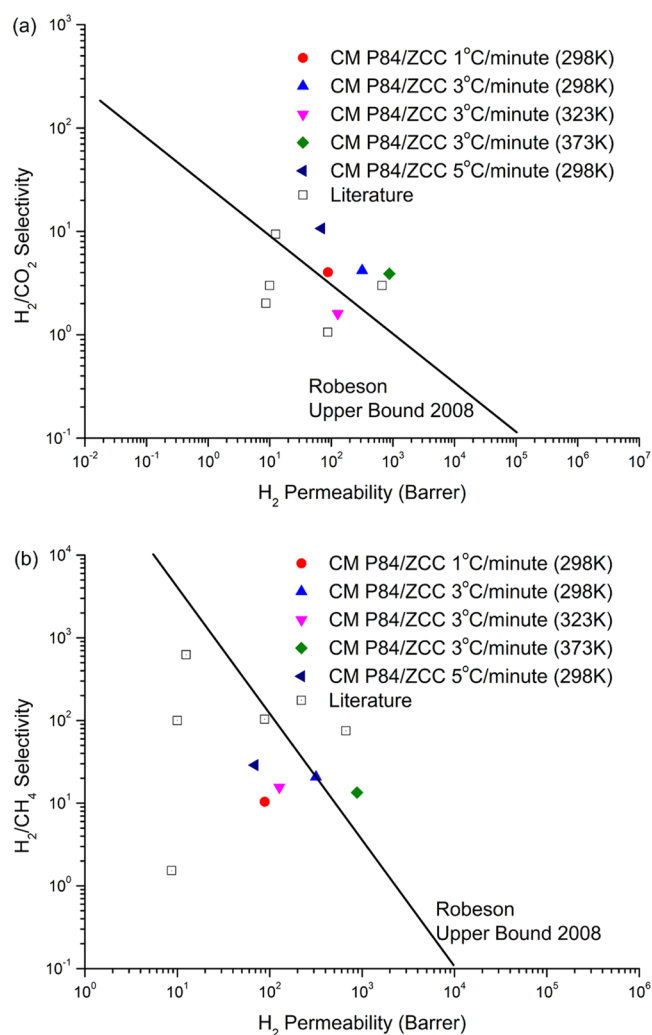
Table 5. Name of Chemical, Structure, and Reason for Selection

| Chemical	Reason for selection	Structure
P84 co-polyimide (BTDA-TDI / MDI) [19]	• High thermal stability • Excellent physical properties • Chemical composition can be changed using a different molecular structure	
Zeolite Composite Carbon [47,48]	• Regular pore structure • High micropore site • Compatibility as carbon membrane filler particles • Sucrose as a precursor due to high carbon yield [49]	Zeolite Y Structure → Zeolite Composite Carbon Structure
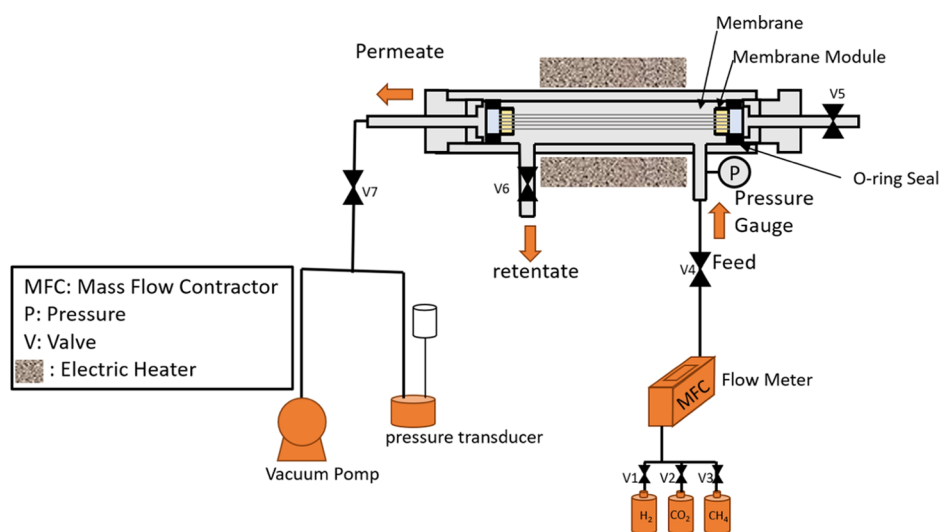
Figure 9. Schematic diagram of the gas permeation rig used in the study.

4.2.2. Membrane Characterization. X-ray diffraction analysis (XRD-Philips PW1140/90) was employed to analyze the *d*-spacing change during the formation of the carbon membrane structure. A field emission scanning electron microscope (JSM-7610F, JEOL) with a potential of 15 kV was used for examining the membrane morphology. The pore properties of the membrane were investigated using a surface area and porosity analyzer (Micromeritics, ASAP 2020).

4.2.3. Gas Permeation Test. Single gas permeation experiments were conducted utilizing H_2, CO_2, and CH_4. Permeation was measured at different permeation temperatures, specifically at 298, 323, and 373 K. Permeation of H_2, CO_2, and CH_4 was measured using bubble flow and pressure difference techniques depending on the permeance recorded. Each gas was permeated from the outside to the inside of the membrane. The feed pressure of the bubble flow was 2.2 bar. More details on both methods can be found elsewhere.[96] The gas permeation rig is illustrated in Figure 9.

The permeability calculation was performed based on the equation from Yoshiura et al.[97] The gas permeance result can be calculated using eq 1

$$P_i = \frac{n_i \times l}{tA\Delta P}$$
(1)

where P_i is the gas permeation in mol/(s m^2 Pa) (1 barrer = 3.35×10^{-16} mol/(s m Pa)), n_i (mol) is the permeated molecules, t (s) is the permeation time (s), ΔP (Pa) is the

pressure differential, l is the length of the thickness (m), and A is the effective membrane surface area (m^2).

4.2.4. Thermodynamics. A thermodynamic study was conducted to define the permeation characteristics of H_2, CO_2, and CH_4 permeating through a carbon membrane. The thermodynamic parameters were determined using the van't Hoff equation (eq 2)

$$\ln \frac{p}{p_0} = \frac{\Delta H}{RT} - \frac{\Delta S}{R}$$
(2)

where ΔH is the enthalpy of permeation (kJ/mol), T is the temperature (K), p is the pressure at the equilibrium state (bar), and R is the gas constant (8.314 J/(mol K)).[49]

4.2.5. Activation Energy. The Arrhenius equation was used for the calculation of activation energy as shown in eq 3

$$\ln P = -\frac{E_a}{RT} + \ln P_0$$
(3)

where E_a is the activation energy (kJ/mol), T is the temperature (K), P is gas permeability (mol/(m s Pa)), P_0 is the pre-exponential factor, and R is the gas constant (8.314 J/(mol K)).[94]

ASSOCIATED CONTENT

Ⓢ Supporting Information

The Supporting Information is available free of charge at https://pubs.acs.org/doi/10.1021/acsomega.1c00512.

Gas permeation result of the P84/ZCC composite carbon membrane with heating rate variations; gas permeation result of the P84/ZCC composite carbon membrane at various permeation temperatures; and P84/ZCC mixed matrix membrane and carbon composite membrane sample images (PDF)

AUTHOR INFORMATION

Corresponding Author

Nurul Widiastuti — *Department of Chemistry, Faculty of Science and Data Analytics, Institut Teknologi Sepuluh Nopember, Surabaya 60111, Indonesia;* ⓞ orcid.org/0000-0002-6821-8116; Phone: +62-31-5943353; Email: nurul_widiastuti@chem.its.ac.id; Fax: +62-31-5928314

Authors

Alvin Rahmad Widyanto — *Department of Chemistry, Faculty of Science and Data Analytics, Institut Teknologi Sepuluh Nopember, Surabaya 60111, Indonesia*

Irmariza Shafitri Caralin — *Department of Chemistry, Faculty of Science and Data Analytics, Institut Teknologi Sepuluh Nopember, Surabaya 60111, Indonesia*

Triyanda Gunawan — *Department of Chemistry, Faculty of Science and Data Analytics, Institut Teknologi Sepuluh Nopember, Surabaya 60111, Indonesia*

Rika Wijiyanti — *Department of Chemistry, Faculty of Science and Data Analytics, Institut Teknologi Sepuluh Nopember, Surabaya 60111, Indonesia*

Wan Norharyati Wan Salleh — *Advanced Membrane Technology Research Center (AMTEC), Universiti Teknologi Malaysia (UTM), 81310 Skudai, Johor Darul Ta'zim, Malaysia;* ⓞ orcid.org/0000-0002-8212-3893

Ahmad Fauzi Ismail — *Advanced Membrane Technology Research Center (AMTEC), Universiti Teknologi Malaysia (UTM), 81310 Skudai, Johor Darul Ta'zim, Malaysia*

Mikihiro Nomura — *Department of Applied Chemistry, Shibaura Institute of Technology, Koto-ku, Tokyo 135-8548, Japan*

Kohei Suzuki — *Department of Applied Chemistry, Shibaura Institute of Technology, Koto-ku, Tokyo 135-8548, Japan*

Complete contact information is available at:
https://pubs.acs.org/10.1021/acsomega.1c00512

Notes

The authors declare no competing financial interest.

ACKNOWLEDGMENTS

REFERENCES

(1) Wassie, S. A.; Cloete, S.; Spallina, V.; Gallucci, F.; Amini, S.; van Sint Annaland, M. Techno-Economic Assessment of Membrane-Assisted Gas Switching Reforming for Pure H2 Production with CO2 Capture. *Int. J. Greenhouse Gas Control* **2018**, *72*, 163−174.

(2) Rostrup-Nielsen, J. R.; Sehested, J.; Nørskov, J. Hydrogen and Synthesis Gas by Steam- and CO_2 Reforming. *Advances in Catalysis*; Academic Press, 2002; Vol. 47, pp 65−139.

(3) Mousavian, S.; Faravar, P.; Zarei, Z.; Azimikia, R.; Ghasemi Monjezi, M.; Kianfar, E. Modeling and Simulation Absorption of CO2 using Hollow Fiber Membranes (HFM) with Mono-Ethanol Amine with Computational Fluid Dynamics. *J. Environ. Chem. Eng.* **2020**, *8*, No. 103946.

(4) Zhao, Y.; Jung, B. T.; Ansaloni, L.; Ho, W. S. W. Multiwalled Carbon Nanotube Mixed Matrix Membranes Containing Amines for High Pressure CO2/H2 Separation. *J. Membr. Sci.* **2014**, *459*, 233−243.

(5) Aydani, A.; Brunetti, A.; Maghsoudi, H.; Barbieri, G. CO2 Separation from Binary Mixtures of CH4, N2, and H2 by Using SSZ-13 Zeolite Membrane. *Sep. Purif. Technol.* **2021**, *256*, No. 117796.

(6) Huang, W.; Jiang, X.; He, G.; Ruan, X.; Chen, B.; Nizamani, A. K.; Li, X.; Wu, X.; Xiao, W. A Novel Process of H2/CO2 Membrane Separation of Shifted Syngas Coupled with Gasoil Hydrogenation. *Processes* **2020**, *8*, No. 590.

(7) Liang, C. Z.; Chung, T. S.; Lai, J. Y. A Review of Polymeric Composite Membranes for Gas Separation and Energy Production. *Prog. Polym. Sci.* **2019**, *97*, No. 101141.

(8) Ismail, A. F.; Khulbe, K. C.; Matsuura, T. *Gas Separation Membranes: Polymeric and Inorganic*; Springer, 2015; pp 1−331.

(9) Wu, Z. Inorganic Membranes for Gas Separations. In *Membrane Separation Principles and Applications*; Ismail, A. F.; Rahman, M. A.; Othman, M. H. D.; Matsuura, T., Eds.; Handbooks in Separation Science; Elsevier, 2019; Chapter 5, pp 147−179.

(10) Ono, R.; Ikeda, A.; Matsuyama, E.; Nomura, M. Permeation Evaluation of a Mordenite Zeolite Membrane by Using an Alkaline Post-Treatment. *J. Chem. Eng. Jpn.* **2015**, *48*, 444−449.

(11) Sugiyama, Y.; Ikarugi, S.; Oura, K.; Ikeda, A.; Matsuyama, E.; Ono, R.; Nomura, M.; Tawarayama, H.; Saito, T.; Kuwahara, K. MFI Zeolite Membranes Prepared on Novel Silica Substrates. *J. Chem. Eng. Jpn.* **2015**, *48*, 891−896.

(12) Song, S.; Gao, F.; Zhang, Y.; Li, X.; Zhou, M.; Wang, B.; Zhou, R. Separation and Puri Fi Cation Technology Preparation of SSZ-13 Membranes with Enhanced Fl Uxes Using Asymmetric Alumina Supports for N2/C4 and CO2/C4 Separations. *Sep. Purif. Technol.* **2019**, *209*, 946−954.

(13) Zong, Z.; Carreon, M. A. Thin SAPO-34 Membranes Synthesized in Stainless Steel Autoclaves for N2/CH4 Separation. *J. Membr. Sci.* **2017**, *524*, 117−123.

(14) Chen, W. H.; Tsai, C. W.; Lin, Y. L. Numerical Studies of the Influences of Bypass on Hydrogen Separation in a Multichannel Pd Membrane System. *Renewable Energy* **2017**, *104*, 259−270.

(15) Zhu, B.; Tang, C. H.; Xu, H. Y.; Su, D. S.; Zhang, J.; Li, H. Surface Activation Inspires High Performance of Ultra-Thin Pd Membrane for Hydrogen Separation. *J. Membr. Sci.* **2017**, *526*, 138−146.

(16) Nayebossadri, S.; Speight, J. D.; Book, D. Hydrogen Separation from Blended Natural Gas and Hydrogen by Pd-Based Membranes. *Int. J. Hydrogen Energy* **2019**, *44*, 29092−29099.

(17) Jo, Y. S.; Lee, C. H.; Kong, S. Y.; Lee, K.-Y.; Yoon, C. W.; Nam, S. W.; Han, J. Characterization of a Pd/Ta Composite Membrane and Its Application to a Large Scale High-Purity Hydrogen Separation from Mixed Gas. *Sep. Purif. Technol.* **2018**, *200*, 221−229.

(18) Rungta, M.; Wenz, G. B.; Zhang, C.; Xu, L.; Qiu, W.; Adams, J. S.; Koros, W. J. Carbon Molecular Sieve Structure Development and Membrane Performance Relationships. *Carbon* **2017**, *115*, 237−248.

(19) Favvas, E. P.; Romanos, G. E.; Katsaros, F. K.; Stefanopoulos, K. L.; Papageorgiou, S. K.; Mitropoulos, A. C.; Kanellopoulos, N. K. Gas Permeance Properties of Asymmetric Carbon Hollow Fiber

Membranes at High Feed Pressures. *J. Nat. Gas Sci. Eng.* **2016**, *31*, 842−851.

(20) Hosseini, S. S.; Chung, T. S. Carbon Membranes from Blends of PBI and Polyimides for N2/CH4 and CO2/CH4 Separation and Hydrogen Purification. *J. Membr. Sci.* **2009**, *328*, 174−185.

(21) Itta, A. K.; Tseng, H.-H.; Wey, M.-Y. Fabrication and Characterization of PPO/PVP Blend Carbon Molecular Sieve Membranes for H2/N2 and H2/CH4 Separation. *J. Membr. Sci.* **2011**, *372*, 387−395.

(22) Matsuyama, E.; Ikeda, A.; Komatsuzaki, M.; Sasaki, M.; Nomura, M. High-Temperature Propylene/Propane Separation through Silica Hybrid Membranes. *Sep. Purif. Technol.* **2014**, *128*, 25−30.

(23) Nomura, M.; Matsuyama, E.; Ikeda, A.; Komatsuzaki, M.; Sasaki, M. Preparation of Silica Hybrid Membranes for High Temperature CO_2 Separation. *J. Chem. Eng. Jpn.* **2014**, *47*, 569−573.

(24) Ikeda, A.; Nomura, M. Preparation of Amorphous Silica Based Membranes for Separation of Hydrocarbons. *J. Jpn. Pet. Inst.* **2016**, *59*, 259−265.

(25) Sanyal, O.; Zhang, C.; Wenz, G. B.; Fu, S.; Bhuwania, N.; Xu, L.; Rungta, M.; Koros, W. J. Next Generation Membranes —Using Tailored Carbon. *Carbon* **2018**, *127*, 688−698.

(26) Salleh, W. N. W.; Ismail, A. F. Effects of Carbonization Heating Rate on CO 2 Separation of Derived Carbon Membranes. *Sep. Purif. Technol.* **2012**, *88*, 174−183.

(27) Li, H.; Haas-santo, K.; Schygulla, U.; Dittmeyer, R. Inorganic Microporous Membranes for H 2 and CO 2 Separation — Review of Experimental and Modeling Progress. *Chem. Eng. Sci.* **2015**, *127*, 401−417.

(28) Karunaweera, C.; Musselman, I. H.; Balkus, K. J.; Ferraris, J. P. Fabrication and Characterization of Aging Resistant Carbon Molecular Sieve Membranes for C3 Separation Using High Molecular Weight Crosslinkable Polyimide, 6FDA-DABA. *J. Membr. Sci.* **2019**, *581*, 430−438.

(29) Hazazi, K.; Ma, X.; Wang, Y.; Ogieglo, W.; Alhazmi, A.; Han, Y.; Pinnau, I. Ultra-Selective Carbon Molecular Sieve Membranes for Natural Gas Separations Based on a Carbon-Rich Intrinsically Microporous Polyimide Precursor. *J. Membr. Sci.* **2019**, *585*, 1−9.

(30) Kamath, M. G.; Fu, S.; Itta, A. K.; Qiu, W.; Liu, G.; Swaidan, R.; Koros, W. J. 6FDA-DETDA: DABE Polyimide-Derived Carbon Molecular Sieve Hollow Fiber Membranes: Circumventing Unusual Aging Phenomena. *J. Membr. Sci.* **2018**, *546*, 197−205.

(31) Gunawan, T.; Romadiansyah, T. Q.; Wijiyanti, R.; Salleh, W. N. W.; Widiastuti, N. Zeolite Templated Carbon: Preparation, Characterization and Performance as Filler Material in Co-Polyimide Membranes For. *Malays. J. Fundam. Appl. Sci.* **2019**, *15*, 407−413.

(32) Sari, P.; Gunawan, T.; Wan Salleh, W. N.; Ismail, A. F.; Widiastuti, N. Simple Method to Enhance O2/N2 Separation on P84 Co-Polyimide Hollow Fiber Membrane. *IOP Conf. Ser.: Mater. Sci. Eng.* **2019**, *546*, No. 042042.

(33) Sazali, N.; Salleh, W. N. W.; Siregar, J. P.; Othman, M. H. D.; Jaafar, J.; Gunawan, T. PI/NCC- Based Carbon Molecular Sieve Membranes for Hydrogen Purification: Effect of Aging Times. *IOP Conf. Ser.: Mater. Sci. Eng.* **2020**, *736*, No. 022003.

(34) Sazali, N.; Mamat, R.; Siregar, J. P.; Gunawan, T.; Salleh, W. N. W.; Nordin, N. A. H. M. PI/NCC Carbon Membrane: Effect of Additives Loading Towards Hydrogen Separation. *IOP Conf. Ser.: Mater. Sci. Eng.* **2020**, *736*, No. 022002.

(35) Lei, L.; Pan, F.; Lindbråthen, A.; Zhang, X.; Hillestad, M.; Nie, Y.; Bai, L.; He, X.; Guiver, M. D. Carbon Hollow Fiber Membranes for a Molecular Sieve with Precise-Cutoff Ultramicropores for Superior Hydrogen Separation. *Nat. Commun.* **2021**, *12*, No. 268.

(36) Wey, M. Y.; Chen, H. H.; Lin, Y. T.; Tseng, H. H. Thin Carbon Hollow Fiber Membrane with Knudsen Diffusion for Hydrogen/ Alkane Separation: Effects of Hollow Fiber Module Design and Gas Flow Mode. *Int. J. Hydrogen Energy* **2020**, *45*, 7290−7302.

(37) Favvas, E. P.; Romanos, G. E.; Papageorgiou, S. K.; Katsaros, F. K.; Mitropoulos, A. C.; Kanellopoulos, N. K. A Methodology for the Morphological and Physicochemical Characterisation of Asymmetric Carbon Hollow Fiber Membranes. *J. Membr. Sci.* **2011**, *375*, 113−123.

(38) Sazali, N.; Salleh, W. N. W.; Ismail, A. F.; Wong, K. C.; Iwamoto, Y. Exploiting Pyrolysis Protocols on BTDA-TDI/MDI (P84) Polyimide/Nanocrystalline Cellulose Carbon Membrane for Gas Separations. *J. Appl. Polym. Sci.* **2019**, *136*, No. 46901.

(39) Favvas, E. P.; Heliopoulos, N. S.; Papageorgiou, S. K.; Mitropoulos, A. C.; Kapantaidakis, G. C.; Kanellopoulos, N. K. Helium and Hydrogen Selective Carbon Hollow Fiber Membranes: The Effect of Pyrolysis Isothermal Time. *Sep. Purif. Technol.* **2015**, *142*, 176−181.

(40) Suda, H.; Haraya, K. Molecular Sieving Effect of Carbonized Kapton Polyimide Membrane. *J. Chem. Soc., Chem. Commun.* **1995**, 1179−1180.

(41) Xu, B.; Zhao, X.; Chen, H.; Su, S.; Yu, H. Effects of Carbonization Conditions on Structure and Gas Adsorption of Carbon Membranes Derived from Polyvinyl Chloride. *ChemistrySelect* **2020**, *5*, 957−961.

(42) Zainal, W. N. H. W.; Tan, S. H.; Ahmad, M. A. Controlled Carbonization Heating Rate for Enhancing CO 2 Separation Based on Single Gas Studies. *Period. Polytech., Chem. Eng.* **2019**, 97−104.

(43) Tseng, H. H.; Shiu, P. T.; Lin, Y. S. Effect of Mesoporous Silica Modification on the Structure of Hybrid Carbon Membrane for Hydrogen Separation. *Int. J. Hydrogen Energy* **2011**, *36*, 15352−15363.

(44) Liu, Q.; Wang, T.; Liang, C.; Zhang, B.; Liu, S.; Cao, Y.; Qiu, J. Zeolite Married to Carbon: A New Family of Membrane Materials with Excellent Gas Separation Performance. *Chem. Mater.* **2006**, *18*, 6283−6288.

(45) Zhang, X.; Hu, H.; Zhu, Y.; Zhu, S. Effect of Carbon Molecular Sieve on Phenol Formaldehyde Novolac Resin Based Carbon Membranes. *Sep. Purif. Technol.* **2006**, *52*, 261−265.

(46) Zhang, B.; Shi, Y.; Wu, Y.; Wang, T.; Qiu, J. Towards the Preparation of Ordered Mesoporous Carbon/Carbon Composite Membranes for Gas Separation. *Sep. Sci. Technol.* **2014**, *49*, 171−178.

(47) Gunawan, T.; Rahayu, R. P.; Wijiyanti, R.; Salleh, W. N. W.; Widiastuti, N. P84/Zeolite-Carbon Composite Mixed Matrix Membrane for CO2/CH4 Separation. *Indones. J. Chem.* **2019**, *19*, 650−659.

(48) Widiastuti, N.; Gunawan, T.; Fansuri, H.; Salleh, W. N.; Ismail, A. F.; Sazali, N. P84/ZCC Hollow Fiber Mixed Matrix Membrane with PDMS Coating to Enhance Air Separation Performance. *Membranes* **2020**, No. 267.

(49) Wijiyanti, R.; Gunawan, T.; Nasri, N. S.; Karim, Z. A.; Ismail, A. F.; Widiastuti, N. Hydrogen Adsorption Characteristics for Zeolite-Y Templated Carbon. *Indones. J. Chem.* **2019**, *20*, No. 29.

(50) Gunawan, T.; Wijiyanti, R.; Widiastuti, N. Adsorption-Desorption of CO2 on Zeolite-Y-Templated Carbon at Various Temperatures. *RSC Adv.* **2018**, *8*, 41594−41602.

(51) Peixoto, I.; Faria, M.; Gonçalves, M. C. Synthesis and Characterization of Novel Integral Asymmetric Monophasic Cellu-lose−Acetate/Silica/Titania and Cellulose−Acetate/Titania Mem-branes. *Membranes* **2020**, *10*, No. 195.

(52) Sazali, N.; Salleh, W. N. W.; Ismail, A. F.; Kadirgama, K.; Moslan, M. S.; Othman, F. E. C.; Ismail, N. H.; Samykano, M.; Harun, Z. Effect of Heating Rates on the Microstructure and Gas Permeation Properties of Carbon Membranes. *Malays. J. Fundam. Appl. Sci.* **2018**, *14*, 378−381.

(53) Gunawan, T.; Widiastuti, N.; Fansuri, H.; Wan Salleh, W. N.; Ismail, A. F.; Lin, R.; Motuzas, J.; Smart, S. The Utilization of Micro-Mesoporous Carbon-Based Filler in the P84 Hollow Fibre Membrane for Gas Separation. *R. Soc. Open Sci.* **2021**, *8*, No. 201150.

(54) He, X.; Lie, J. A.; Sheridan, E.; Hagg, M. B. Preparation and Characterization of Hollow Fiber Carbon Membranes from Cellulose Acetate Precursors. *Ind. Eng. Chem. Res.* **2011**, *50*, 2080−2087.

(55) Geiszler, V. C.; Koros, W. J. Effects of Polyimide Pyrolysis Conditions on Carbon Molecular Sieve Membrane Properties. *Ind. Eng. Chem. Res.* **1996**, *35*, 2999−3003.

(56) Jaya, M. A. T.; Harun, W. M. H. F. W.; Ahmad, M. A. Influence of Pyrolysis Temperature and Heating Rate in the Fabrication of Carbon Membrane: A Review. *J. Appl. Sci.* **2014**, *14*, 1359−1364.

(57) Yoshimune, M.; Fujiwara, I.; Haraya, K. Carbon Molecular Sieve Membranes Derived from Trimethylsilyl Substituted Poly (Phenylene Oxide) for Gas Separation. *Carbon* **2007**, *45*, 553−560.

(58) Kim, Y. K.; Park, H. B.; Lee, Y. M. Gas Separation Properties of Carbon Molecular Sieve Membranes Derived from Polyimide/Polyvinylpyrrolidone Blends: Effect of the Molecular Weight of Polyvinylpyrrolidone. *J. Membr. Sci.* **2005**, *251*, 159−167.

(59) Yang, Z.; Peng, H.; Wang, W.; Liu, T. Crystallization Behavior of Poly(ε-Caprolactone)/Layered Double Hydroxide Nanocomposites. *J. Appl. Polym. Sci.* **2010**, *116*, 2658−2667.

(60) Campo, M. C.; Magalhães, F. D.; Mendes, A. Comparative Study between a CMS Membrane and a CMS Adsorbent: Part I — Morphology, Adsorption Equilibrium and Kinetics. *J. Membr. Sci.* **2010**, *346*, 15−25.

(61) Qiao, X.; Chung, T.-S. Diamine Modification of P84 Polyimide Membranes for Pervaporation Dehydration of Isopropanol. *AIChE J.* **2006**, *52*, 3462−3472.

(62) Sazali, N.; Salleh, W.; Ismail, A.; Ismail, N.; Yusof, N.; Aziz, F.; Jaafar, J.; Nordin, N. Controlled Dip-Coating Times for Improving CO2 Selective of PI/NCCbased Supported Carbon Membrane. *J. Membr. Sci. Technol.* **2018**, *8*, No. 1000178.

(63) Shen, Y.; Lua, A. C. Effects of Membrane Thickness and Heat Treatment on the Gas Transport Properties of Membranes Based on P84 Polyimide. *J. Appl. Polym. Sci.* **2010**, *116*, 2906−2912.

(64) Tin, P. S.; Chung, T. S.; Liu, Y.; Wang, R. Separation of CO2/CH4 through Carbon Molecular Sieve Membranes Derived from P84 Polyimide. *Carbon* **2004**, *42*, 3123−3131.

(65) Su, J.; Lua, A. C. Effects of Carbonisation Atmosphere on the Structural Characteristics and Transport Properties of Carbon Membranes Prepared from Kapton Polyimide. *J. Membr. Sci.* **2007**, *305*, 263−270.

(66) Hamm, J. B. S.; Ambrosi, A.; Griebeler, J. G.; Marcilio, N. R.; Tessaro, I. C.; Pollo, L. D. Recent Advances in the Development of Supported Carbon Membranes for Gas Separation. *Int. J. Hydrogen Energy* **2017**, *42*, 24830−24845.

(67) Marriott, A. S.; Hunt, A. J.; Bergström, E.; Thomas-Oates, J.; Clark, J. H. Effect of Rate of Pyrolysis on the Textural Properties of Naturally-Templated Porous Carbons from Alginic Acid. *J. Anal. Appl. Pyrolysis* **2016**, *121*, 62−66.

(68) Burggraaf, A. J. Single Gas Permeation of Thin Zeolite (MFI) Membranes: Theory and Analysis of Experimental Observations. *J. Membr. Sci.* **1999**, *155*, 45−65.

(69) Sea, B.-K.; Watanabe, M.; Kusakabe, K.; Morooka, S.; Kim, S.-S. Formation of Hydrogen Permselective Silica Membrane for Elevated Temperature Hydrogen Recovery from a Mixture Containing Steam. *Gas Sep. Purif.* **1996**, *10*, 187−195.

(70) Shelekhin, A. B.; Dixon, A. G.; Ma, Y. H. Theory of Gas Diffusion and Permeation in Inorganic Molecular-Sieve Membranes. *AIChE J.* **1995**, *41*, 58−67.

(71) Gilron, J.; Soffer, A. Knudsen Diffusion in Microporous Carbon Membranes with Molecular Sieving Character. *J. Membr. Sci.* **2002**, *209*, 339−352.

(72) Sotomayor, F. J.; Cychosz, K. A.; Thommes, M.; Sotomayor, F.; Cychosz, K. A.; Thommes, M. Characterization of Micro/Mesoporous Materials by Physisorption: Concepts and Case Studies Characterization of Micro/Mesoporous Materials by Physisorption: Concepts and Case Studies. *Acc. Mater. Surf. Res.* **2018**, *3*, 34−50.

(73) Gaabour, L. H. Thermal Spectroscopy and Kinetic Studies of PEO/PVDF Loaded by Carbon Nanotubes. *J. Mater.* **2015**, *2015*, No. 824859.

(74) Centeno, T. A.; Fuertes, A. B. Supported Carbon Molecular Sieve Membranes Based on a Phenolic Resin. *J. Membr. Sci.* **1999**, *160*, 201−211.

(75) Wang, C.; Hu, X.; Yu, J.; Wei, L.; Huang, Y. Intermediate Gel Coating on Macroporous Al2O3 Substrate for Fabrication of Thin Carbon Membranes. *Ceram. Int.* **2014**, *40*, 10367−10373.

(76) Yong, W. F.; Lee, K.; Chung, T.; Weber, M.; Staudt, C. Blends of a Polymer of Intrinsic Microporosity and Partially Sulfonated Polyphenylenesulfone for Gas Separation. *ChemSusChem* **2016**, 1953−1962.

(77) Centeno, T. A.; Vilas, J. L.; Fuertes, A. B. Effects of Phenolic Resin Pyrolysis Conditions on Carbon Membrane Performance for Gas Separation. *J. Membr. Sci.* **2004**, *228*, 45−54.

(78) Song, C.; Wang, T.; Wang, X.; Qiu, J.; Cao, Y. Preparation and Gas Separation Properties of Poly(Furfuryl Alcohol)-Based C/CMS Composite Membranes. *Sep. Purif. Technol.* **2008**, *58*, 412−418.

(79) Chen, X.; Hong, L.; Chen, X.; Yeong, W. H. A.; Chan, W. K. I. Aliphatic Chain Grafted Polypyrrole as a Precursor of Carbon Membrane. *J. Membr. Sci.* **2011**, *379*, 353−360.

(80) Tseng, H.-H.; Shiu, P.-T.; Lin, Y.-S. Effect of Mesoporous Silica Modification on the Structure of Hybrid Carbon Membrane for Hydrogen Separation. *Int. J. Hydrogen Energy* **2011**, *36*, 15352−15363.

(81) Yin, X.; Chu, N.; Yang, J.; Wang, J.; Li, Z. Thin Zeolite T/Carbon Composite Membranes Supported on the Porous Alumina Tubes for CO2 Separation. *Int. J. Greenhouse Gas Control* **2013**, *15*, 55−64.

(82) Li, G.; Yang, J.; Wang, J.; Xiao, W.; Zhou, L.; Zhang, Y.; Lu, J.; Yin, D. Thin Carbon/SAPO-34 Microporous Composite Membranes for Gas Separation. *J. Membr. Sci.* **2011**, *374*, 83−92.

(83) Koros, W. J.; Zhang, C. Materials for Next-Generation Molecularly Selective Synthetic Membranes. *Nat. Mater.* **2017**, *16*, 289−297.

(84) Oyama, S. T.; Yamada, M.; Sugawara, T.; Takagaki, A.; Kikuchi, R. Review on Mechanisms of Gas Permeation through Inorganic Membranes. *J. Jpn. Pet. Inst.* **2011**, *54*, 298−309.

(85) Yoshimune, M.; Haraya, K. CO$_2$/CH$_4$ Mixed Gas Separation Using Carbon Hollow Fiber Membranes. *Energy Procedia* **2013**, *37*, 1109−1116.

(86) Au, L. T. Y.; Yin Mui, W.; Sze Lau, P.; Tellez Ariso, C.; Yeung, K. L. Engineering the Shape of Zeolite Crystal Grain in MFI Membranes and Their Effects on the Gas Permeation Properties. *Microporous Mesoporous Mater.* **2001**, *47*, 203−216.

(87) Bernal, M. P.; Coronas, J.; Menéndez, M.; Santamaría, J. Characterization of Zeolite Membranes by Temperature Programmed Permeation and Step Desorption. *J. Membr. Sci.* **2002**, *195*, 125−138.

(88) Lai, Z.; Tsapatsis, M. Gas and Organic Vapor Permeation through B-Oriented MFI Membranes. *Ind. Eng. Chem. Res.* **2004**, *43*, 3000−3007.

(89) Poshusta, J. C.; Noble, R. D.; Falconer, J. L. Temperature and Pressure Effects on CO2 and CH4 Permeation through MFI Zeolite Membranes. *J. Membr. Sci.* **1999**, *160*, 115−125.

(90) Tseng, R. L.; Wu, F. C.; Juang, R. S. Adsorption of CO2 at Atmospheric Pressure on Activated Carbons Prepared from Melamine-Modified Phenol-Formaldehyde Resins. *Sep. Purif. Technol.* **2015**, *140*, 53−60.

(91) Acharya, N. K.; Yadav, P. K.; Vijay, Y. K. Study of Temperature Dependent Gas Permeability for Polycarbonate Membrane. *Indian J. Pure Appl. Phys.* **2004**, *42*, 179−181.

(92) Tondeur, D.; Kvaalen, E. Equipartition of Entropy Production. An Optimality Criterion for Transfer and Separation Processes. *Ind. Eng. Chem. Res.* **1987**, *26*, 50−56.

(93) Lasseuguette, E.; Malpass-Evans, R.; Carta, M.; McKeown, N. B.; Ferrari, M. C. Temperature and Pressure Dependence of Gas Permeation in a Microporous Tröger's Base Polymer. *Membranes* **2018**, *8*, No. 132.

(94) Fu, S.; Sanders, E. S.; Kulkarni, S.; Chu, Y. H.; Wenz, G. B.; Koros, W. J. The Significance of Entropic Selectivity in Carbon Molecular Sieve Membranes Derived from 6FDA/DETDA:DABA(3:2) Polyimide. *J. Membr. Sci.* **2017**, *539*, 329−343.

(95) Robeson, L. M. The Upper Bound Revisited. *J. Membr. Sci.* **2008**, *320*, 390−400.

(96) Myagmarjav, O.; Ikeda, A.; Tanaka, N.; Kubo, S.; Nomura, M. Preparation of an H2-Permselective Silica Membrane for the Separation of H2 from the Hydrogen Iodide Decomposition Reaction

in the Iodine−Sulfur Process. *Int. J. Hydrogen Energy* **2017**, *42*, 6012−6023.

(97) Yoshiura, J.; Ishii, K.; Saito, Y.; Nagataki, T.; Nagataki, Y.; Ikeda, A.; Nomura, M. Permeation Properties of Ions through Inorganic Silica-Based Membranes. *Membranes* **2020**, *10*, No. 27.